ISSN 1063-7842, Technical Physics, 2006, Vol. 51, No. 7, pp. 919–923. © Pleiades Publishing, Inc., 2006.
Original Russian Text © E.B. Aleksandrov, A.K. Vershovskiĭ, A.S. Pazgalev, 2006, published in Zhurnal Tekhnicheskoĭ Fiziki, 2006, Vol. 76, No. 7, pp. 103–107.

EXPERIMENTAL INSTRUMENTS AND TECHNIQUES

Magnetometer Based on a Pair of Symmetric Transitions in the ^{87}Rb Hyperfine Structure

E. B. Aleksandrov, A. K. Vershovskiĭ, and A. S. Pazgalev

Ioffe Physicotechnical Institute, Russian Academy of Sciences,
Politekhnicheskaya ul. 26, St. Petersburg, 194021 Russia
e-mail: antver@mail.ioffer.ru

Received December 28, 2005

Abstract—A new version of the fast optically pumped magnetometer, an optically pumped balanced quantum magnetometer, built around a pair of symmetric transitions in the hyperfine structure of the ^{87}Rb ground state is implemented for the first time. The noise-limited sensitivity of the prototype in terms of the variance is 6 pT for a measurement time of 0.1 s. The basic advantages of the new magnetometer are the absence of dead zones when it changes orientation relative to the magnetic field and an extremely low sensitivity to the drift of pumping parameters.

PACS numbers: 07.55.Ge
DOI: 10.1134/S1063784206070176

PROBLEM DEFINITION

An optically pumped quantum magnetometer (OPQM) based on the microwave resonance in the hyperfine structure (HFS) of the ground state of an alkali metal atom was proposed in the 1970s [1, 2]. It was also shown at the time that the use of the resonance between magnetic sublevels belonging to different hyperfine levels provides a number of advantages over the OPQM's standard scheme (where the resonance between two magnetic sublevels of the same hyperfine level is employed). For example, by specially tailoring the configuration of the microwave field, the HFS magnetometer (HFSM) can be made free of dead zones, i.e., capable of functioning at any angles between the optical pump axis and magnetic field vector. In addition, the systematic error of such a magnetometer can be reduced to a level of 1 pT. However, to achieve these goals, it is necessary to eliminate the effect of light- and collision-induced shifts of atomic levels, as well as the drift of the reference oscillator in the microwave range or, in other words, to accomplish the balanced modification of the device so that it can measure the frequencies of transitions between two symmetric pairs of magnetic levels (for example, $F = 2$, $m_F = -2 \rightleftharpoons F = 1$, $m_F = -1$ and $F = 2$, $m_F = 2 \rightleftharpoons F = 1$, $m_F = 1$). In such an approach, the difference between the frequencies of two transitions in the HFS bears information about the magnetic field strength. One more advantage of the device considered is that it can operate in a very wide range of magnetic fields from extremely weak fields (down to 200 nT) to fields on the order of several tens of oersteds.

At the same time, the performance of the HFSM is inferior to that of the conventional OPQM in several respects. First, the former detects resonances in the occupations of magnetic sublevels (M_Z resonances), i.e., is inferior to M_X devices in speed. Second, the need to operate in the microwave range and also to simultaneously measure the frequencies of two transitions significantly complicates the design of the device's electronics.

An attempt to obviate these disadvantages was made in [3]. It was suggested that, instead of two independent microwave transitions, two transitions sharing the same upper level be excited. Such transitions constitute the Λ scheme featuring the effect of coherent trapping of occupations [4].

In this work, we for the first time describe a magnetometer utilizing transitions in the HFS of the ^{87}Rb ground state that is designed on the symmetric balanced scheme. The device is intended for measuring the magnetic field magnitude at a rate of up to 10 cps. The balanced scheme is implemented on transitions with frequencies F_0^- ($F = 2$, $m_F = -2 \rightleftharpoons F = 1$, $m_F = -1$) and F_0^+ ($F = 2$, $m_F = 2 \rightleftharpoons F = 1$, $m_F = 1$),

$$F_0^+ = F_0 + 3/4F_0x + 3/16F_0x^2 - 3/32F_0x^3 + \ldots,$$

$$F_0^- = F_0 - 3/4F_0x + 3/16F_0x^2 + 3/32F_0x^3 + \ldots.$$

Here, $x = (g_J + g_I)\mu_B/(hF_0)B$, μ_B is the Bohr magneton, h is the Planck constant, $\mu_B/h \approx 13.996246$ GHz/T, $g_J = 2.002331$ and $g_I = 0.998823 \times 10^{-3}$ are the electronic

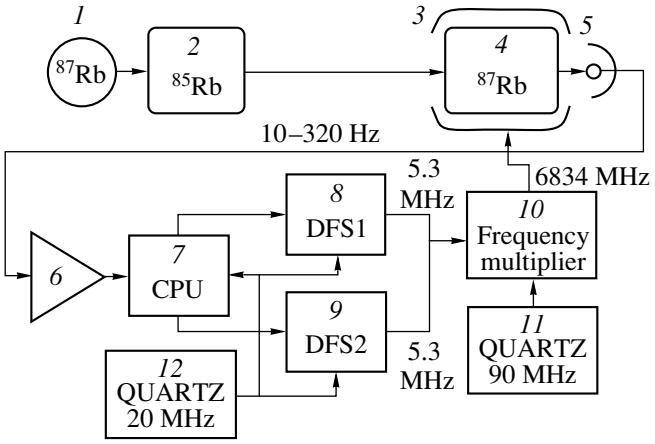

Fig. 1. Schematic of the HFS magnetometer: (*1*) lamp with ^{87}Rb vapor, (*2*) isotope filter, (*3*) microwave cavity, (*4*) cell, (*5*) photodetector, (*6*) photocurrent amplifier, (*7*) central processor unit, (*8*, *9*) digital frequency synthesizers, (*11*) high-stability 90-MHz reference oscillator, and (*12*) 20-MHz reference oscillator.

and nuclear g factors of the ^{87}Rb isotope, $F_0 \approx$ 6834.683 MHz is the frequency of the transition in the HFS without the magnetic field, and B is the magnetic induction. The difference frequency of these two transitions, $F^{\mathrm{d}} = F_0^+ - F_0^- = 3/2F_0x - 3/16F_0x^3$, varies with the field almost linearly. The cubic term, which in a mean terrestrial field of 50 μT is small (≈11 mHz (0.26 pT)) can be neglected, which greatly simplifies data processing. Frequency F^{d} is six times more sensitive to a magnetic field (a sensitivity of about 42 Hz/nT) than the frequency of the transition between two neighboring magnetic sublevels. This means that, all other things being equal, the sensitivity can be raised by a factor of $6/\sqrt{2} = 4.24$ (the square root appears if noise in the two channels is assumed to be uncorrelated).

OPERATION OF THE DEVICE

The block diagram of the device is shown in Fig. 1. The ^{87}Rb HFS is optically pumped by the isotopic filtering method. The nonpolarized light of a ^{87}Rb lamp passes through a filter, which is a heated cell containing ^{85}Rb vapor. A pumping radiation enters a sensor through a multiple-fiber guide. The sensor contains a buffer-gas-filled 50-mm-long cylindrical cell 40 mm in diameter, which is placed in an open cavity (part of a cylindrical waveguide matched to a transmitting antenna). The cavity with the cell is, in turn, placed in a thermostat kept at 45°C.

The magnetic resonance linewidth measured under the operating conditions was 6–7 nT (200–300 Hz); the optical pumping power was 30–40 μW (λ = 780 and 795 nm); and the microwave power delivered to the sensor, 200–300 μW.

The signals of M_Z resonances are detected with a low-frequency photodetector, which receives the light coming from the sensor through the light guide, and processed by a multiprocessor unit. The electronics of the system (specifically, frequency synthesizers and signal processors) is all-digital (except for the input photocurrent amplifier). So, low-frequency analog electronics is absent: synchronous detectors and integrators, which are routinely used in resonance-tracking systems, are replaced by a 10-bit ADC, which controls two 48-bit frequency synthesizers. The use of the microprocessor and controlled frequency synthesizers in the feedback loop allows measurement of two magnetic resonance frequencies with an accuracy of 10^{-8}.

Along with serving the function of frequency-locked tuning, the microprocessor fulfills such functions as initial search and locking of both resonances, averaging and display of the measurements, monitoring of the current state of the units, execution of user commands, etc. The control of the device and data acquisiton/processing functions are performed with a specially devised programmable interface. To excite the magnetic resonance signal in the ^{87}Rb HFS, it is necessary to synthesize two microwave signals symmetrically offset (accurate to 1 Hz) from frequency F_0. The synthesis is based on balanced modulation of a high-frequency reference signal. Low-frequency digital synthesizers generate signals F_1 and F_2 with frequencies near 5.3 MHz, which are then mixed with a reference signal frequency of 90 MHz multiplied by 76 times ($F_H = 76 \cdot 90 = 6840$ MHz) to produce a microwave field containing two frequencies, $F^+ = F_H - F_1$ and $F^- = F_H - F_2$. The feedback loops bring these frequencies to resonance with frequencies F_0^+ and F_0^- of the respective transitions.

The frequency of the quartz-crystal reference oscillator was taken as high as possible (90 MHz) to minimize phase noise attendant to frequency multiplication [5]. The instability of frequency F_H (on the order of 10^{-7}) has a negligible effect on the long-term stability of the magnetometer, because the synthesis scheme is balanced. However, the instability of the oscillator used to clock the frequency synthesizers contributes to the long-term stability (absolute error) of the device. With this in mind, we introduced an additional highly stable 20-MHz quartz-crystal oscillator (featuring a long-term drift of 10^{-8}–10^{-7} per day, which corresponds to an absolute error of 0.5–5.0 pT in measuring magnetic fields of 50 μT) in order to synchronize the microprocessor and frequency synthesizers. Provision is also made in the device to synchronize the frequency synthesizers by means of an external highly stable oscillator at frequencies of 5, 10, and 20 MHz (for example, by means of a frequency standard).

To simultaneously detect signals due to two HFS transitions in a single optical channel, we applied rectangular frequency modulation of both resonance com-

ponents of the microwave field in such a way that modulation frequency f_{mod} was the same in both channels and the modulation phases in the channels were shifted by 90°. This and also the fact that both signals pass through the same low-frequency section provide the same dynamic response of the channels and, hence, balance of the scheme. The signal from the photodetector is digitized, and, by appropriately selecting the reference voltage phase, one can discriminate the signals (transitions) at frequencies F^+ and F^- and, thereby, create two independent feedback loops. It should be noted that the analog low-frequency section is identical for both tracking loops, since it contains nothing but the photocurrent amplifier, which is shared by the loops; therefore, the phase delay in them is also the same.

The algorithm of the microprocessor involves synchronous detection with sliding primary integration strictly over one modulation period $1/f_{mod}$. This makes it possible to exclude the second harmonic at frequency $2f_{mod}$ in the frequency-locked loop and substantially raise the speed of the device (to $\tau = 1/f_{mod}$ in the limit).

As in any M_Z magnetometer, the presence of the modulation frequency second harmonic in the signal channel of the balanced magnetometer indicates the presence of the M_Z resonance signal. If, however, modulation is sinusoidal and the modulation phases are shifted by 90°, two second harmonics of two identical resonance lines (at frequency $2f_{mod}$) become 180° out of phase and, thereby, quench each other. This problem may be obviated by using nonsinusoidal modulation signals. Figure 2 shows the modulation signal waveforms and the respective signals at the center of the resonance lines. The basic idea of such a way of modulation is to discriminate between the time instants the first or second channel generates a microwave field that is in resonance with transitions F_0^+ and F_0^- and the time instants both fields are out of resonance with these transitions. To this end, the modulation period was divided into eight phases (Figs. 2a, 2b) so that the above condition is fulfilled for each of them with the modulation signals in either channel strictly symmetric and phase-shifted by 90° at resonance locking (Figs. 2c–2e). Figure 2f shows the experimental shape of the resonance signal detected at the first and second modulation harmonics in one channel.

One reason for the systematic error in the M_Z magnetometer is modulation asymmetry. In our case, the modulation half-period was kept constant accurate to two clock cycles of the microprocessor (1 clock cycle = 0.1 μs). For a modulation frequency of 160 Hz and a linewidth of 8 nT, the associated error equals 0.25 pT. The modulation frequency in our experiments can be varied from 10 to 640 Hz.

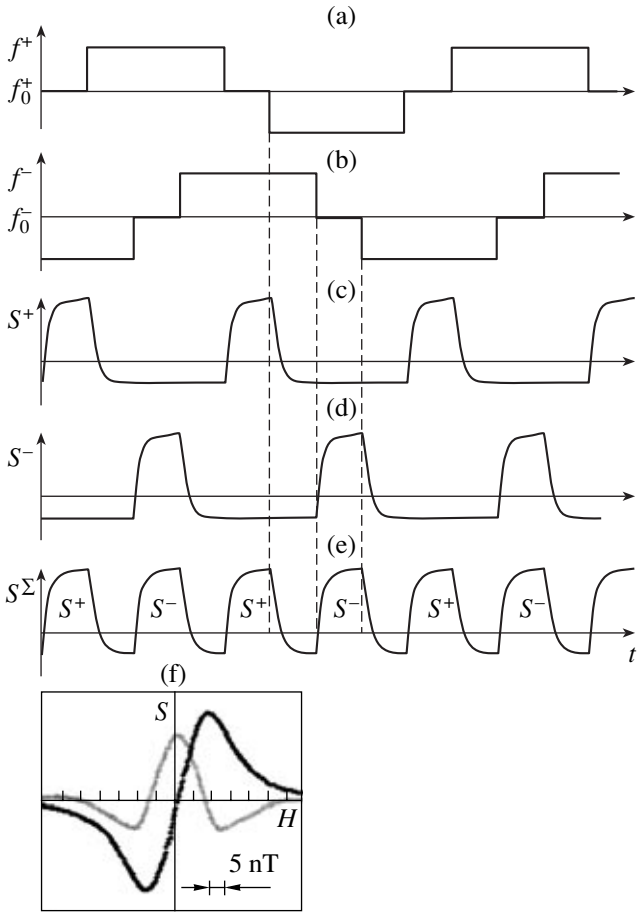

Fig. 2. Time waveforms of (a, b) modulation of resonance microwave fields, (c, d) respective signals at the center of the resonance lines, and (e) the net signal at locking of both channels. (f) Shows the resonance signal in one channel at the first and second modulation harmonics.

EXPERIMENT

In the first series of experiments, the prototype of the magnetometer was surrounded by a three-layer Permalloy screen within which a magnetic field of induction 6000 nT was maintained. The basic parameters responsible for the magnetic resonance signal quality (the temperatures of the sensor cell and isotope filter, the microwave field applied to the sensor, the operating conditions of the lamp, and the optical pumping intensity) were optimized. Also, we tested the operating compatibility and dynamics of two feedback loops and the performance of the resonance locking algorithm (i.e., observed how the device switches to the frequency-locked tuning regime). The parameters of the sensors were optimized so as to maximize the HFS resonance quality factor (the ratio of the signal amplitude to the resonance linewidth times the noise spectral amplitude at the resonance frequency). Finally, we optimized the parameters of the feedback loops so that the spread of the magnetic field measured by the device

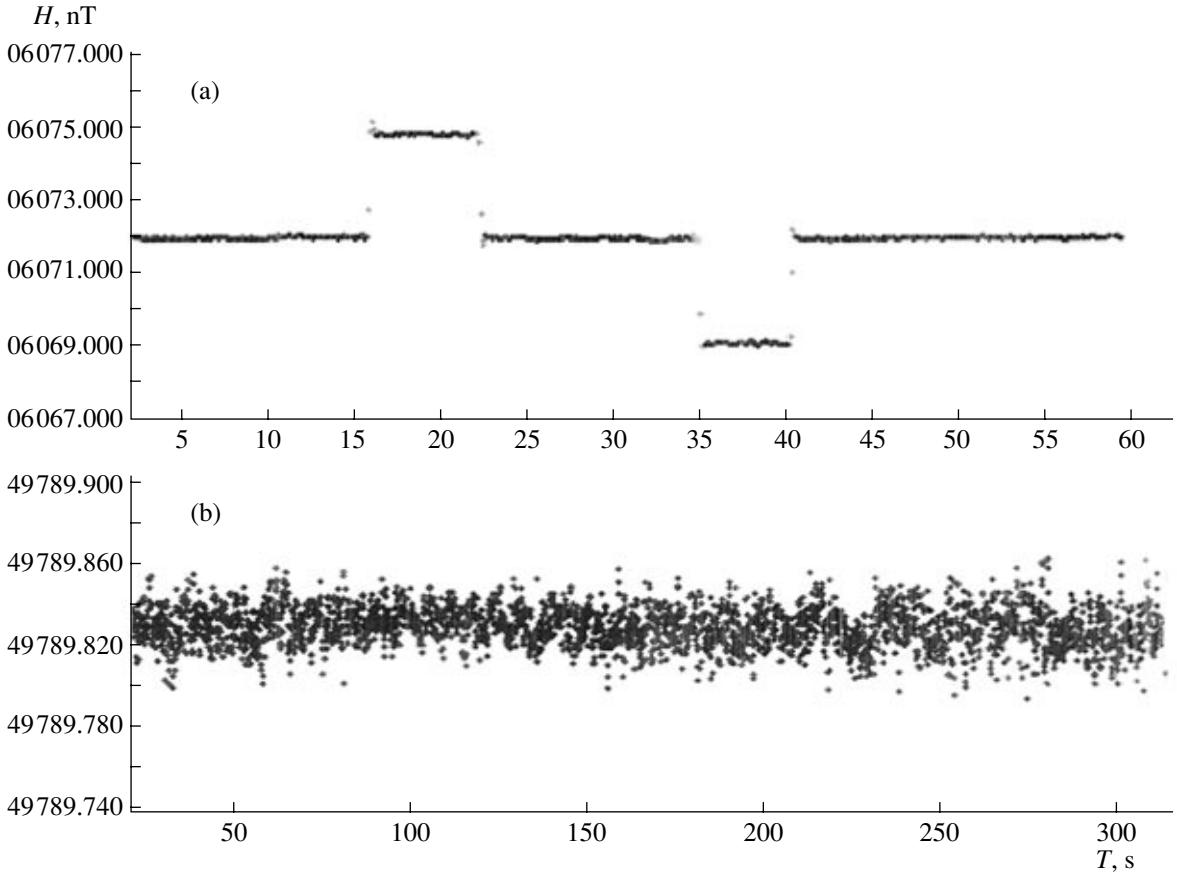

Fig. 3. Records made with the HFS magnetometer (10 cps). (a) Field recorded in the screen: the response of the device to a step change in the field and (b) field recorded in the stabilizer. The vertical scale is 20 pT/div.

was as small as possible at a given speed (no less than 10 cps, see Fig. 3a).

In the second series of tests, the prototype was placed in a magnetic field stabilizer that is a constituent of the magnetic induction primary standard at the Mendeleev All-Russia Institute of Metrology. Our goals were to determine the short-term sensitivity of the prototype and its speed, measure parameter-related drifts, and check the performance of the prototype in the magnetic induction range 20–80 μT. Magnetic induction records made during the tests are exemplified in Fig. 3b. For the parameters of the frequency-locked loop providing a speed of 0.1 s (Fig. 3a), the device offers a short-term sensitivity of 6.0 pT in terms of the variance at a measurement time of 0.1 s, 5.3 pT at a measurement time of 1 s, and 2.5 pT at a measurement time of 10 s. As was expected, the sensitivity is limited by microwave noise. The drift of readings was also measured. It was found that the component proportional to the optical pumping intensity (optical drift) is at least no higher than the measurement sensitivity and so does not affect the readings. At the same time, technical drift ΔH_t arising in response to variation of any parameter (pumping intensity I_p, microwave amplitude H_1, cell temperature T_c, etc.) decreases the signal amplitude. In all the cases, ΔH_t nonlinearly grows with decreasing signal second harmonic amplitude S, and the dependence $\Delta H_t(S)$ is approximated well by the relationship $\Delta H_t = 0.018/[S/S_0]^2$, where S_0 is the second harmonic amplitude at optimal parameters. The technical drift can be explained if we assume that harmonics making a constant contribution to the resonance signal exist in the vicinity of the resonance. At a modulation frequency of 80 Hz, these may be main harmonics at 50 and 100 Hz. At $S = S_0$, the total value of the technical drift is $\Delta H_{t0} = 18$ pT. The total drift of readings (the sum of technical and other drifts) is no more than ±10 pT at $|\Delta I_p| \le 10\%$, $|\Delta H_1| \le 20\%$, and $|\Delta T_c| \le 0.6$°C.

The device is free of dead zones. When the angle between the sensor and horizontal changed from 0° to 90°, the relative change in the second harmonic amplitude was no higher than 30%. The orientation drift of amplitude 0.5 nT is due to the remanent magnetization of the prototype's sensor.

We are planning long-term experiments aimed at comprehensively studying the long-term stability and drifts of the device.

CONCLUSIONS

The performance of a new fast optically pumped magnetometer is demonstrated. The magnetometer is built around a pair of symmetric transitions in the ^{87}Rb hyperfine structure. Its noise-limited sensitivity in terms of the variance is 6 pT at a measurement time of 0.1 s.

ACKNOWLEDGMENTS

The authors thank V.Ya. Shifrin and E.N. Choporova for assistance in conducting the experiments.

REFERENCES

1. E. B. Aleksandrov and A. B. Mamyrin, Izmer. Tekh. **20**, 73 (1977).
2. E. B. Aleksandrov, A. B. Mamyrin, and N. N. Yakobson, Zh. Tekh. Fiz. **51**, 607 (1981) [Sov. Phys. Tech. Phys. **26**, 363 (1981)].
3. A. K. Vershovskii, E. B. Aleksandrov, and A. V. Pazgalev, Zh. Tekh. Fiz. **70** (1), 88 (2000) [Tech. Phys. **45**, 88 (2000)].
4. E. Arimondo and E. Wolf, Prog. Opt. **35**, 257 (1996).
5. E. B. Aleksandrov, A. K. Vershovskii, A. S. Pazgalev, and N. N. Yakobson, Zh. Tekh. Fiz. **60** (9), 58 (1990) [Sov. Phys. Tech. Phys. **25**, 1034 (1990)].

Translated by V. Isaakyan